Serotype survey of AAV gene delivery via subconjunctival injection in mice

Liujiang Song[1,2,3], **Telmo Llanga**[2,3], **Laura M. Conatser**[2,3], **Violeta Zaric**[2], **Brian C. Gilger**[4], **Matthew L. Hirsch**[2,3]

[1]School of Medicine, Hunan Normal University, Changsha 422800 Hunan, China

[2]Gene Therapy Center, University of North Carolina at Chapel Hill, Chapel Hill, NC 27599, USA

[3]Department of Ophthalmology, University of North Carolina, Chapel Hill, Chapel Hill, NC 27599, USA

[4]Department of Clinical Sciences, North Carolina State University, Raleigh, NC 27607, USA

Abstract

AAV gene therapy approaches in the posterior eye resulted in the first FDA-approved gene therapy-based drug. However, application of AAV vectorology to the anterior eye has yet to enter even a Phase I trial. Furthermore, the simple and safe subconjunctival injection has been relatively unexplored in regard to AAV vector transduction. To determine the utility of this route for the treatment of various ocular disorders, a survey of gene delivery via natural AAV serotypes was performed and correlated to reported cellular attachment factors. AAV serotypes packaged with a self-complementary reporter were administered via subconjunctival injection to WT mice. Subconjunctival injection of AAV vectors was without incidence; however, vector shedding in tears was noted weeks following administration. AAV transduction was serotype dependent in anterior segment tissues including the eye lid, conjunctiva, and cornea, as well as the periocular tissues including muscle. Transgene product in the cornea was highest for AAV6 and AAV8, however, their corneal restriction was remarkably different; AAV6 appeared restricted to the endothelium layer while AAV8 efficiently transduced the stromal layer. Reported AAV cellular receptors were not well correlated to vector transduction; although, in some cases they were conserved among mouse and human ocular tissues. Subconjunctival administration of particular AAV serotypes may be a simple and safe targeted gene delivery route for ocular surface, muscular, corneal, and optic nerve diseases.

Introduction

Anterior segment eye diseases encompass a broad range of genetic and/or acquired disorders that include dry eye disease, corneal fibrosis/angiogenesis, and Fuchs dystrophy. Due to the relatively easy accessibility via several administration routes and the compartmentalization of the eye from the body, anterior segment eye diseases are inherently attractive targets for local drug delivery. However, despite the recent FDA approval of the first commercial gene therapy for an ocular posterior disease, Leber's Congenital Amaurosis (LCA) [1, 2], gene delivery based on adeno-associated virus (AAV) to various tissues in the anterior segment is relatively unexplored, especially following subconjunctival injection. Compared to corneal intrastromal or intracameral drug administration, subconjunctival injections are simple, safe, and are administered to patients with only local anesthesia usually in an out-patient setting [3]. Given the administration route dependence by a single serotype and serotype-dependent transduction following a single administration route [4], the potential for subconjunctival gene delivery to specific ocular tissues is a formal possibility, thereby expanding the therapeutic repertoire for the treatment of anterior segment eye diseases.

AAV is a small single-stranded DNA virus initially discovered in 1965 as a contaminant of an adenovirus preparation [5, 6]. In 1980s, it was known that all viral coding sequences could be substituted by transgenic DNA, and if the viral genes are provided in *trans* alongside other "helper" genes, AAV vectors (harboring the transgenic DNA) are produced [7, 8]. The last 30 years have realized "bench to bedside" for AAV gene therapy for several diseases and in 2017, the FDA approved the first commercial gene therapy drug, based on AAV, for the treatment of a posterior segment ocular disorder. The success of AAV vectors, compared to other viral and non-viral gene delivery approaches is in part due to: (i) its extremely infectious nature for most human tissues, (ii) AAV vector genomes (vg) persist as episomes with low levels of host integration, (iii) serotypes display altered tropisms, (iv) the ability to infect dividing or non-dividing cells, and (v) preclinical and clinical data demonstrating transgene expression for many years following a single administration. AAV has emerged as, perhaps, the most promising gene delivery vector and has been clinically applied to diverse diseases via different routes of administration; however, it has yet to be applied for the therapy of an anterior segment eye disease in humans.

Although specific anterior segment eye disease etiologies and manifestations exist requiring disease-targeted gene delivery, there are five administration routes described for anterior segment AAV gene delivery including: (i) topical [9–17], (ii) corneal intrastromal [18, 19], (iii) intracameral [20–24], (iv) lacrimal gland injections [25], and (v) subconjunctival [26–28]. AAV administration based on the later route has not been adequately explored with only three reports described in the literature. In 2007, two separate publications demonstrated that AAV serotype 2 (AAV2) packaged with angiostatin or endostatin cDNA administered days prior to a corneal burn inhibited corneal angiogenesis [26, 28]. However, vector transduction of particular cell types and different ocular tissues was poorly characterized. In contrast to these promising reports, in 2013, Igarashi et al. reported that subconjunctival injection of AAV8 resulted in no reporter expression in the compartments examined in the eye; however, strong liver and periocular transduction were noted [27]. Therefore, many questions regarding vector genome biodistribution, transgene expression/abundance, safety, serotype-

dependent tropism, and importantly, relevance to disease therapy remain to be answered. Therefore, in the present study, we analyzed the transduction efficiency, the biodistribution, serum immunogenicity, tissue specificity, and the safety of three natural AAV serotypes administered by subconjunctival injection in mice. In this study, AAV serotypes 2, 6, and 8 were chosen due to their historical significance, altered cellular receptor reliance, and their popularity in clinical trials [29–31]. The results demonstrate serotype-dependent tropisms supporting the relevance of AAV gene therapy via subconjunctival injection for diseases of the ocular anterior segment.

Results

Evaluation of the safety of subconjunctival injection of AAV

To define the site of drug administration following subconjunctival injections used in this study, 14 μl of diluted India ink or PBS were administered subconjunctivally to anesthetized 10-month-old mice with no obvious backflow, leaking, or bleeding observed during or following the injections. Twenty minutes post-injection, ocular and surrounding tissues were prepared for Hematoxylin and Eosin (H&E) staining to determine ink distribution. Representative sagittal and transverse plane sections indicate India ink dispersion existed mainly in the periocular loose connective tissues, at the outer surface of the sclera, and posterior to the eye adjacent to extraocular muscles (Fig. 1). Notably, the side injected had more dye than the non-injected side.

Next, self-complementary AAV vector preparations harboring a cytomegalovirus promoter driven enhanced green fluorescent protein reporter (CMV-GFP) cassette were thoroughly characterized by Southern dot blotting, quantitative polymerase chain reaction (qPCR) (for titer), alkaline gel electrophoresis (for packaged vector genome integrity), and silver staining (Fig. S1). AAV vectors (7×10^9 vg) or PBS (negative control) were injected subconjunctivally in C57BL/6J mice as described for the India ink injections. No leakage was observed and resolution of conjunctival distension occurred within minutes with no observed complications.

Three weeks post-injections, slit lamp examination revealed no abnormal discharge or corneal edema, although vascularization and focal cornea opacification was observed in approximately 50% of both control and AAV-injected mice. These corneal changes were reported to develop spontaneously or be induced by ketamine/xylazine anesthesia in C57BL/6J mice [32, 33]. No significant body weight changes were observed in the experiment ($p > 0.05$, $n = 3$, Fig. S2. A). Alanine aminotransferase (ALT) levels were not significant different from the PBS control mice at 2 weeks post-injection ($p > 0.05$, $n = 3$), although an increase in ALT was observed 8 weeks post-injection, the significance was not determined (Fig. S2. B). Tear production determined by a phenol red thread test (PRT) did not show significant differences between AAV-injected and control mice ($p > 0.05$, $n = 6$, Fig. 2a). The general morphology of the eye structures, the degree of cellular infiltrates, fibrosis, and the extent of neovascularization of both the cornea and conjunctiva/episcleral area were graded on the H&E-stained sections, and no significant difference was observed ($p > 0.05$, $n = 3$, Fig. S2. C).

AAV vector shedding, or dissemination of AAV vectors, from the treated patient is commonly noted in clinical AAV gene therapy sometimes over a period >6 months [29, 34]. Detection of potential vector shedding in tears following subconjunctival injections was performed via PCR amplification and radioactive probe hybridization at weeks 1 and 4 post-injection. As shown in Fig. 2b, at the earlier time point post-injection, 1 of 6 tear samples in AAV2 group, 3 of 6 tear samples in AAV6 group, and 2 of 6 samples in AAV8 group showed vector genome-specific bands. No vector genomes were detected in tear samples collected 30 days post-injection. In a few instances, β-actin was also detected in our tear samples (Fig. S3).

Tropism of AAV capsid serotypes following subconjunctival injection in WT mice

Eight weeks post-injection, immunofluorescence staining was used to examine GFP abundance in whole globe cross-sections. The results demonstrate that AAV vectors administered via subconjunctival injection efficiently transduce the periocular muscles posterior to the eye, irrespective of capsid serotypes (Fig. 3a), which correlates to the India ink distribution pattern after subconjunctival injection (Fig. 1). As shown in Fig. 3a, little to no GFP expression was observed in eyelid, conjunctival fornix, trabecular meshwork, or retina by immunofluorescence. As for the cornea, GFP detection by immunofluorescene was not detectable in AAV2-treated mice. Interestingly, GFP abundance in the AAV6-injected group appeared mostly restricted to the endothelium, along with occasional low-level expression in the stroma, while strong GFP signal was present in the stroma but not in the epithelium or endothelium of AAV8-treated eyes. To better localize the GFP expression in the cornea, three-dimensional confocal immunofluorescence Z-stack images with a step of 0.60 μm under 63×/1.4 oil objectives were acquired. As presented in Fig. 3b, GFP was highly restricted to the endothelium in AAV6- and the stroma in AAV8-treated animals, whereas GFP was barely detectable in the AAV2 group.

AAV vector biodistribution and transgene expression following subconjunctival injection

In addition to transgene product immunofluorescence, vector genome biodistribution in distinct ocular tissues, draining submandibular lymph nodes, and peripheral organs was determined 2 months following subconjunctival injection of AAV serotypes. Notably, AAV2, AAV6, and AAV8 all showed the highest vector copy number in the conjunctiva (about 10^5 vg/μg), and showed a significant number of vector genomes in the eyelid, cornea, third eyelid ($n = 4$) and the submandibular lymph nodes ($n = 3$) ($p < 0.05$) compared to the PBS-injected group. Although AAV8 viral genome copy number exceeded 10^4 vg/μg of gDNA in all selected tissues, AAV6 viral genome exceeded 10^4 vg/μg only in the cornea and optic nerve (Fig. 4a). AAV6 and AAV8, but not AAV2, were also detected in the retina and optic nerve. As shown in the Fig. 4a, vector genomes were below or close to the limit of the detection in the salivary gland, liver, and heart.

To identify the most efficient capsid serotype for ocular tissues after subconjunctival injection, we next quantitatively analyzed actual transduction, or transgene expression (cDNA, Fig. 4b). In all cases, no reverse transcriptase controls were employed to eliminate concerns of DNA contamination in our RNA preparations. As shown in Fig. 4b, AAV8 and AAV6 vectors demonstrated significant transduction in the eyelid, conjunctiva, optic nerve,

and cornea (vs. PBS group, $p < 0.05$, $n = 4$). Notably, AAV2 and AAV6 had an equal amount of genomes in the cornea ($p = 0.4857$, $n = 4$), but AAV6 showed significantly higher transduction than AAV2 ($p = 0.0286$, $n = 4$). Although a significant number of genomes in the conjunctiva and cornea were detected (vs. PBS group, $p < 0.05$, $n = 4$), the AAV2 subconjunctival injections resulted in minimal to no transduction in all selected tissues. None of the serotypes showed significant gene expression in the third eyelid, retina, or submandibular lymph nodes ($p > 0.05$, $n = 4$), (Fig. 4b). In general, these data suggest that the capsid serotype affects both the overall vector biodistribution, as well as the transgene expression levels.

Neutralizing antibody analysis

The presence of antibodies targeted to AAV capsids is a concern for patient candidate selection in AAV gene therapy trials due to their ability to neutralize transduction. In the mice of this study, a broad range of serum dilutions (1:1–1:2048) were analyzed for neutralizing antibody activity and the data indicate that injected animals mounted a strong humoral response. In particular, the titer of the neutralizing antibody (Table 1) for AAV2 was the most robust (1:2048), while reduced titers were noted for AAV6 (1:256–1:1024) and AAV8 (1:128–1:256). These results indicate that subconjunctival injection consistently generates an anti-AAV capsid humoral response in mice under the tested conditions.

AAV receptor analysis in mouse and human corneas

In an effort to rationalize the different transgene biodis-tribution/expression patterns mediated by different serotypes in the cornea and, importantly, for the potential translation from murine to man, we examined the expression of the reported cellular receptors for AAV in both mouse and human corneas by immunofluorescence. As shown in Fig. 5a, different capsid serotypes are reported to preferentially interact with different and/or overlapping primary/secondary receptors [35–42]. As presented in Fig. 5b, heparin sulfate proteoglycan (HSPG) [35], as the first identified receptor for AAV2 and 6, showed positive staining at the interface between the endothelial layer and Descemet's layer in mouse corneas. The staining of epidermal growth factor receptor (EGFR) [37], reported as an AAV6 receptor, was strong, continuous, and appeared localized to the cell surface throughout the epithelium layer, with the strongest staining intensity in the basal layers in both mouse and human corneas (Fig. 5b). The expression of 37/67 kDa laminin receptor (Lam R) [39], a putative receptor of AAV2 and 8, was observed in all epithelium, stromal, and endothelium layers in both mouse and human corneas (Fig. 5b). A recently identified "universal receptor" for AAV2, 6, and 8, AAVR [38], was found in human cornea layers, and to a lesser degree in the epithelium and endothelium layer of mouse corneas (Fig. 5b). Lectin staining with Wheat Germ Agglutinin (WGA, binds sialic acid in any linkage), Sambucus Nigra Lectin (SNA, binds α2, 6 N-linked sialic acid), and Maackia Amurensis Lectin I (MAL I, recognizes α2, 3 N-linked sialic acid) was performed since α2, 3 and α2, 6 N-linked sialic acid [41] have been suggested to be the attachment receptors for AAV6. There is high expression of sialic acid throughout the mouse and human cornea, but the α2, 3 N-linked sialic acid was solely in the endothelium layer. No obvious staining was observed for α2, 6 staining. As shown in Fig. S4, EGFR, 37/67 kDa Lam R, AAVR, and sialic acid were also present in the conjunctiva in mice, while the 37/67 kDa Lam R, AAVR, HSPG as well as sialic

acid were also detected in mouse retina. In short, these data suggest that, although the AAV receptor expression patterns share similarities between mouse and human corneas, the different transgene expression pattern may not entirely be attributed to the AAV receptor expression; thus the underlining mechanism remains to be further investigated.

Discussion

Despite the success in the ocular posterior segment, AAV gene therapy has never entered into even a Phase I trial for any anterior ocular disease. Regarding drug administration to this compartment, topical application is seemingly the most attractive; however, without prior corneal epithelial debridement, AAV gene delivery by this route is minimal [10, 11, 43] (data not shown). Corneal intrastromal and intracameral injections of AAV vectors have also been well characterized and demonstrate impressive serotype-dependent transduction of different anterior eye compartments [18–24]; however, both of these administration routes induce transient corneal damage, and are not commonly used in the clinic. In contrast, subconjunctival injections are common, simple, and are performed with only topical anesthesia. Furthermore, based on previous MRI studies [44] and Fig. 1, subconjunctival injections distribute to a large periocular space, and are already in use for drug delivery to different target tissues, including the retina and optic nerve [45]. Despite these attributes, AAV vector transduction following subconjunctival injection remains poorly characterized and a whole globe/periocular analysis comparing different AAV serotypes did not exist. Herein, it is demonstrated that subconjunctival AAV vector administration was well tolerated with no ocular or systemic clinical abnormalities. AAV vector shedding in tears was detected for minimally a week following the injection; however, no vectors were detected at 1 month post-injection. Postmortem results on mouse eyes demonstrate transgene expression in the eyelid, conjunctiva, cornea, optic nerve, and extraocular muscles. As hypothesized, and shown for other tissues [4], the transduction pattern and vector genome biodistribution, was dependent upon the AAV capsid. In an effort to rationalize serotype-specific transduction to known capsid cellular attachment factors and/or receptors, and to increase translational relevance, six reported receptors/coreceptors were stained in mouse and human corneas. The results demonstrate that AAV serotype-specific transduction did not simply correlate to receptor expression, suggesting that other aspect(s) of the AAV vector infection pathway limit transduction (i.e., nuclear trafficking). Although systemic vector genome biodistribution was minimal 2 months post-injection, antibodies to the injected capsid were generated and capable of inhibiting cognate vector transduction in vitro. Following a one-time simple subconjunctival injection, the results demonstrate AAV serotype-dependent distribution and transduction of several ocular tissues including the cornea, conjunctiva, eyelid, muscle, and the optic nerve.

Vector administration was without incident and overall, there were no indications of vector-induced pathology. Of importance is that our shedding data demonstrate that about one-third of the tear samples collected 1 week post-injection were positive for AAV vector DNA independent of the serotype. Although long-term vector shedding is tolerated, without patient isolation restrictions, in AAV clinical applications, results from systemic AAV Phase I trials and our data raise environmental and safety concerns [29, 34]. Shedded AAV vectors have the potential to deliver transgenic DNA to non-intended recipients which would likely

vaccinate the bystander to the AAV vector capsid and, depending on the bystander's genetics and the transgene, could result in pathology. This is an especially important consideration given the external nature of the anterior eye and concerns of vector mobilization [46], underscoring additional concerns of topical AAV vector application to the eye.

Unlike topical administration following epithelial debridement or intrastromal injections [13], little is known about AAV vector biodistribution/transduction pattern for subconjunctival injections. To the best of our knowledge, there have been only three studies in which AAV vectors were administered via subconjunctival injection. Two reports, over a decade ago, demonstrated the inhibition of burn-induced corneal neovascularization following AAV2-angiostatin [26] or AAV2-endostatin [28] pretreatment by subconjunctival injection. Despite the implication that the transgene product is functional in the peripheral/central cornea, correlation of the therapeutic result to the presence of the transgene product angiostatin or endostatin by histological staining was not presented [26]. Therefore, it remains a mystery as to where AAV2 transduction occurred in these studies [28]. In a 2013 report, AAV8 transduction, using luciferase live imaging, was noted following subconjunctival injection primarily in the liver (likely via the scleral venous sinus), and to a lesser extent in periocular tissue, consistent with our data [27]. Using histology, the same publication noted GFP+ cells in the orbital side tissue, including muscle, following AAV8 subconjunctival injection [27]; however, ocular transduction was not observed in this context. Consistent with that report, our evaluations failed to detect transgene abundance in the optic nerve, retina, or any other posterior ocular tissue using immunofluorescence. In contrast, GFP+ signal was observed in a serotype-dependent manner, throughout the cornea, a region not examined in previous publications [26–28]. Transgene expression in the cornea was confirmed using quantitative reverse-transcription PCR (qRT-PCR), and significant detection was also noted in the optic nerve, conjunctiva, and eyelid. As expected, all of these distinct compartments also contained significant levels of vector genomes, with the conjunctiva, closest to the site of injection, demonstrating the highest value. The sensitivity of PCR perhaps explains, along with substantial ocular autofluorescence, detection in particular compartments (such as eyelid) while immunofluorescence remained negative/inconclusive. Regarding the 2013 report that observed the liver as the primary target of AAV8 transduction following subconjunctival injection [27], we too detected viral genomes in the liver post-injection, however at a very low frequency. Our analysis was at 2 months, a time where reporter expression was almost completely lost [27], and herein coincided with an increase in ALT consistent with the timing of a transgene-dependent CTL-mediated eradication of transduced liver cells [47, 48]. From a clinical perspective, the detection of vector genomes in the liver following subconjunctival injection, even if not significant herein, is consistent to the observed humoral response to the AAV capsid thereby generating concerns of off-target expression and the uncertainty of transduction following repeated subconjunctival vector administration. In the case of AAV vectors injected to the vitreous, a capsid-specific antibody response is elicited that blocks transduction of vectors repeatedly injected to the same space [49–51]. A capsid-specific antibody response is avoided by subretinal injection, and therefore, so is neutralization of repeated subretinal vector administration [49]. Future experiments will determine if the humoral response to

the AAV capsid following subconjunctival delivery will inhibit transduction upon repeat administration.

One of the more dramatic findings was the pattern of cornea transduction among different serotypes: (i) stroma-specific expression (AAV8) and (ii) endothelial-specific expression (AAV6). Considering subconjunctival administration, the "gateway(s)" to the cornea remains unknown, although conceptually, it could be entry at the corneal scleral junction (limbus) or via the anterior chamber. In support of the later is the observation that subconjunctival injections result in anterior chamber dissemination [44]. Consistently, reports have noticed cornea endothelia and stroma transduction following intracameral injection [22, 24]. The reported cellular receptors for AAV serotypes do not offer simple receptor-usage-dependent explanations. Although not observed under the conditions employed herein, the ability of AAV vectors to transduce limbal stem cells and derived epithelial "progenitor" cells is under active investigation.

The expectation of a direct correlation between transduction and the presence of cellular receptors for AAV capsids is sophomoric as the functional roles of these receptors in AAV entry remain unknown. Additionally, AAV vector transduction relies on multiple processes post-entry and despite over three decades of study, aspects of vesicle trafficking, nuclear entry, capsid uncoating, and intranuclear genome localization remain poorly characterized, and perhaps cell type and/or species dependent. At a basic level, associations can be made to explain for instance, AAV6's preference for the endothelium (and not AAV8) could be attributed to the presence of $\alpha2, 3$ sialic acid [41], which is also conserved in human corneal endothelium. However, further studies are necessary to better correlate reported AAV receptors/attachment factors to transduction and the data herein provide an initial roadmap for both mice and human in the cornea as well as more popular gene delivery target, the retina.

In short, our results demonstrate that subconjunctival injection of AAV vectors elicits significant transgene expression in the eyelid, conjunctiva, cornea, and optic nerve. Additionally, extraocular tissues such as eye muscle were also targets of all serotypes tested herein. AAV6 vectors transduce the endothelium layer at a surprisingly high level and AAV8 showed high transduction of the stromal layer. Depending on the target tissue involved in specific diseases, as well as the type of the therapeutic gene, the choice of serotype and the suitability of the subconjunctival injection should be taken into consideration. For example, one of the most common ocular surface ailments, dry eye disease, encompasses multiple anterior eye compartments including the eyelid, conjunctiva, and the cornea [52]. For this disease, one may consider AAV8 delivered by subconjunctival injection, along with an anti-inflammatory transgene, perhaps HLA-G [53], as a viable treatment. Alternatively, Fuch's dystrophy affects the corneal endothelial cells, and based on the results herein, AAV6 vectors administered via subconjunctival injection may transduce the only relevant corneal cell type. Collectively, the AAV survey data herein serve as a foundation for selection and the further development of AAV vectors for ocular disorders following a simple and safe subconjunctival injection.

Methods

Animals

All animals were handled in accordance with the NIH "principles of laboratory animal care" and in compliance with the Association for Research in Vision and Ophthalmology (ARVO) guidelines for the use of animals in ophthalmic and vision research. Additionally, animal use in this study was approved and monitored by the University of North Carolina Institutional Animal Care and Use Committee. Eighteen C57BL/6J mice of both sexes and aged 10 months were randomly divided into groups (PBS, India ink, and AAV), six eyes/group. Mouse serum for neutralizing antibody and ALT analysis was obtained from the sub-mandibular vein before subconjunctival injection and 2 and 8 weeks post-injection and stored at −80 °C. The tears were collected during PRT. Slit lamp examination assessed ocular abnormalities such as ocular hyperemia, cornea opacity, and discharge induced by the injections. Animal were sacrificed 8 weeks following the single subconjunctival injection (unless otherwise stated) and tissues were harvested for further analyses. All experiments were performed without eliminating any mice.

AAV vector production and characterization

Self-complementary AAV-CMV-GFP vectors, provided by the Vector Core at University of North Carolina, were used in this study. In short, vectors harboring the Inverted Terminal Repeats (ITRs) of AAV2 and the capsids from different serotypes were generated via a triple plasmid transfection protocol in HEK293 cells. The AAV particles were purified by iodixanol gradients (OptiPrep Density Gradient Medium; Sigma-Aldrich), followed by ion exchange chromatography using anion exchange. qPCR using SYBR green (Applied Biosystem) and Southern dot blotting with an P^{32} labeled probe were employed to check the titers of the vector genome (vg) [54, 55]; viral purity was assessed by sodium dodecyl sulfate–polyacrylamide gel electrophoresis (SDS–PAGE) followed by silver staining using a kit (ThermoScientific) [56]. Viral genome integrity was accessed by alkaline gel electrophoresis followed by SYBR Gold staining (Molecular Probes, Eugene, OR, USA) [57].

Subconjunctival administration

After the mice were anesthetized by intraperitoneal injection of ketamine at 70 mg/kg (Henry Schein NDC 0409–2051-05), xylazine at 7 mg/kg (Akorn NDC 59399–110-20), and acepromazine at 1.5 mg/kg (Henry Schein NDC 11695–0079-8) in sterile water, topical anesthesia was applied to the eyes using proparacaine 0.1% (Allergan Inc., Irvine, CA). Subconjunctival injections were then performed under an operating microscope and the injection volume and speed/pressure remained constant by using an injector system consisted of a Standard Infuse/Withdraw Pump 11 Pico Plus Elite Programmable Syringe Pump (Harvard Bioscience), a polyethylene tubing (I.D. 0.38 mm, O.D. 1.09 mm) connected to a Hamilton syringe (Hamilton) and a 32G stainless steel needle. Fourteen microliters of PBS, 25% India ink, or viral suspension containing 7×10^9 vg was administered into the temporal quadrant of the bulbar conjunctiva at 200 nl/s. Topical ointment GenTeal (Alcon NDC 0078–0429-47) was applied to the ocular surface after injection to prevent desiccation and the mice were kept warm until fully awake.

Tear production and vector shedding analysis

Tear production was measured by a modified PRT test. Briefly, the bent tip of a Zone-Quick phenol red thread (FCI Ophthalmics, Pembrooke, MA) was placed at the lower conjunctiva fornix and held in place with sterile forceps for 10 s. Upon removal of the thread, the wetted length of the red thread was measured and recorded. The wet portion of the thread containing the tear sample was then cut and placed in 10 mM Tris buffer and stored at −80 °C. Vector shedding through tears after subconjunctival administration was analyzed by two-rounds of standard PCR using GFP primer set (Forward primer 5′AGCAGCACGACTTCTTCAAGTCC3′, Reverse primer 5′TGTAGTTGTACTCCAGCTTGTGCC3′) and a mouse β-actin primer set (Forward primer 5′ TGGCACCACACCTTCTACAAT3′; Reverse primer 5′ AGGCATACAGGGACAGCACA3′) followed by standard agarose electrophoresis and Southern blotting using a P^{32}-labeled probe targeting GFP.

AAV biodistribution

To investigate the biodistribution of AAV vectors delivered via subconjunctival injection, the tissue was harvested at experimental conclusion (8 weeks) following a strict tissue collection and cleaning procedures to minimize the potential of cross-contamination. Upon collection, tissues were frozen on dry ice and then stored at −80 °C. DNA from the heart and liver were isolated using DNeasy Blood and Tissue Kit (Qiagen, Valencia, CA). DNA/RNA from the eyelid, conjunctiva, cornea, retina, optic nerve, third eyelid, submandibular lymph nodes, and salivary glands were extracted with the AllPrep DNA/RNA Mini Kit according to the kit protocol (Qiagen, Valencia, CA). Vector biodistribution was quantitatively analyzed by qPCR utilizing the Taqman probe technology. In short, the amount of vector-specific SV40 genome copies was standardized against an amplicon from a single copy mouse gene, lamin B2, amplified from genomic DNA. For the detection of vector genomes, the plasmid (AAV-CMV-GFP) standard curve was generated by serial ten-fold dilutions in 10 Mm Tris-HCl. qPCR was carried out with an initial denaturation step at 95 °C for 10 min, followed by 45 cycles of denaturation at 95 °C for 10 s, and annealing/extension at 60 °C for 45 s using SV40 polyA primers (forward primer 5′-AGCAATAGCATCACAAATTTCACAA-3′; reverse primer 5′-C CAGACATGATAAGATACATTGATGAGTT-3′) and an internal fluorescent probe (5′-fam AGCATTTTTTTCACTGCATTCTAGTTGTGGTTTGTC tamra-3′). Genomic qPCR of mouse lamin B2 was performed with LightCycler® 480 SYBR Green I Master with the following primers: forward primer 5′-GGACCCAAGGACTACCTCAAGGG-3′; reverse primer 5′-AGGGCACCTCCATCTCGGAAAC-3′. Purified and quantified mouse genomic DNA was used as a standard. The qPCR was carried out with an initial denaturation step at 95 °C for 10 min, followed by 45 cycles of denaturation at 95 °C for 10 s, and annealing first 5 cycles at 64 °C for 10 s then followed by a touch down PCR with a decrease of 2 °C every cycle for 10 s until it reaches the annealing at 60 °C for 10 s in the rest of the cycles. Extension was performed at 72 °C for 10 s. A melting curve analysis was performed at the end to ensure that a single product was amplified. Vector biodistribution data are reported as the number of double-stranded vector DNA (SV40) copies per μg of gDNA.

Quantification of transgene expression by qRT-PCR

Transgene expression was quantitatively analyzed by qRT-PCR. Isolated RNA was subjected to DNase I treatment (Ambion by life technology) before reverse transcription was performed. cDNA was then synthesized with the Second Strand Synthesis Kit (Invitrogen, Carlsbad, CA) in the presence (+RT) and absence (−RT) of reverse transcriptase. qPCR amplification was performed with the same protocol as described above using SV40 primers and specific probe detection. PCR of mouse β-actin was performed with SYBR Green I with the same β-actin primer set mentioned above, and the amplified products were validated by performing a post-PCR melting curve analysis. Standard curves for the transgene was generated by performing ten-fold dilutions of plasmid templates from 5 pg to 0.05 fg mixed with equal amount of cDNA from negative control mice. A standard curve for β-actin was generated by two-fold dilutions of cDNA from negative control mice. When the qPCR result of the samples came out beyond the range of the standard curve, repeated qPCR with further dilution of cDNA samples was performed. When the result was below the lowest detection limit, the results were considered as negative. The results are presented as the transcript copy number/copy of host β-actin. All qRT-PCR and genomic qPCR reactions in this study were performed with a Roche 480 Lightcycler.

AAV neutralizing antibody assay

To determine if subconjunctival injection of AAV vectors results in an antibody response to the injected capsid, a neutralizing antibody assay was performed on HEK 293 cells using a previously reported method [53, 58]. In short, cells were seeded in a 48-well plate at 50,000 cells/well in duplicate on the day before performing vector transduction. The next day, the pre- and 8-week post-injection serum was used 1:1 and then serially diluted 1:2–1:2048 in PBS to a final volume of 13 μl and incubated with AAV-CMV-Firefly Luciferase of the same capsid as what was injected in 13 μl PBS for 2 h at 4 °C. Serum/vector mixture was then added to the cells and a luciferase assay was performed 48 h post-transduction using Promega Luciferase Assay System (Bright-Glo; Promega, Madison, WI) using a Perkin Elmer Victor 3 1420 Multi-label Counter Luminometer. Results were plotted to find the point at which the serum dilution suppressed transduction to less than 50% of pre-injection serum levels. This experiment was repeated at least three times. No pre-existing neutralizing antibodies were detected in any of the mice.

Histology and immunofluorescence for transgene expression and receptor analysis

India ink-injected mice were sacrificed and decapitated at 20 min post-subconjunctival injection. The mouse heads were then subjected to an overnight fixation in 10% formalin and a 24-h decalcification in formic acid solution. Mouse heads were then cut in half sagittally and processed following standard histology protocols. Two eyes from PBS and each AAV group were excised, fixed, embedded in paraffin, and then sectioned at a thickness of 5 μm using a microtome. Routine H&E staining and quantification of cornea histopathology scoring was performed using the previously reported scale (ranging from 0 to 4) [53] and the cumulative scores were presented as mean ± standard deviation (SD). Immunofluorescence was performed following a previously described method [53]. In short, sections were deparaffinized by incubating the slides two times in xylene for 10 min each,

followed by immersing the slides sequentially in two rounds of 100% (3 min each), 95% (1 min), and 80% (1 min) ethanol solutions, and finally in water for 5 min. Antigen retrieval procedure was performed by heating the slides to 95 °C in citrate-based (pH 6.0) antigen unmasking buffer (Vector Laboratories) before staining. Non-specific staining was blocked by using PBS containing 10% of normal goat serum, 0.025% Triton X-100 plus 1% BSA before overnight incubation with the primary antibody. The GFP primary antibody (1:500, AVES labs Inc.) and goat anti-chicken secondary antibody (Alexa Fluor® 488, 1:1000, Abcam) were used to locate GFP expression, while other primary antibodies and their targets follow: anti-EGFR for the detection of EGFR (1:100, Abcam), anti-67 kDa Lam R antibody for 37/67 kDa Lam R (1:100, Abcam), anti-heparin sulfate for HSPGs (1:50, 10E4 clone, Amsbio), anti-KIAA0319L antibody for AAVR (1:100, Proteintech), and goat anti-mouse IgG H&L (Alexa Fluor® 488) or goat anti-rabbit IgG H&L (Alexa Fluor® 594) secondary antibodies were used to assess AAV receptor expression in mouse and human corneas. The following fluorescein-labeled lectins obtained from Vector Laboratories (Burlingame, CA) were used for the staining of specific carbohydrate residues that serve as AAV receptor/coreceptors: WGA for multivalent sialic acid, SNA for α2, 6 sialic acid, and MAL I for α2, 3 sialic acid. After the staining, slides were mounted and counter stained with ProLong™ Diamond Antifade Mountant with DAPI (p36971, Invitrogen) and observed by Olympus IX83 Fluorescence Microscope (Olympus, Tokyo, Japan) or Zeiss LSM 780 inverted confocal microscope.

Statistical analysis

Statistical analysis was performed by using the unpaired Mann–Whitney test using the GraphPad Prism version 7.0c software (GraphPad Software, San Diego, CA, USA), difference was accepted as a p value < 0.05.

Supplementary Material

Refer to Web version on PubMed Central for supplementary material.

Acknowledgements

References

1. Bainbridge JW, Smith AJ, Barker SS, Robbie S, Henderson R, Balaggan K, et al. Effect of gene therapy on visual function in Leber's congenital amaurosis. N Engl J Med. 2008;358:2231–9. [PubMed: 18441371]

2. Feuer WJ, Schiffman JC, Davis JL, Porciatti V, Gonzalez P, Koilkonda RD, et al. Gene therapy for Leber hereditary optic neuropathy: initial results. Ophthalmology. 2016;123:558–70. [PubMed: 26606867]

3. Chong RS, Su DH, Tsai A, Jiang Y, Htoon HM, Lamoureux EL, et al. Patient acceptance and attitude toward an alternative method of subconjunctival injection for the medical treatment of glaucoma. J Glaucoma. 2013;22:190–4. [PubMed: 22036716]

4. Salganik M, Hirsch ML, Samulski RJ. Adeno-associated virus as a mammalian DNA vector. Microbiol Spectr. 2015;3:1–32.

5. Atchison RW, Casto BC, Hammon WM. Adenovirus-associated defective virus particles. Science. 1965;149:754–6. [PubMed: 14325163]

6. Atchison RW, Casto BC, Hammon WM. Electron microscopy of adenovirus-associated virus (AAV) in cell cultures. Virology. 1966;29:353–7. [PubMed: 5943543]

7. Samulski RJ, Srivastava A, Berns KI, Muzyczka N. Rescue of adeno-associated virus from recombinant plasmids: gene correction within the terminal repeats of AAV. Cell. 1983;33:135–43. [PubMed: 6088052]

8. Srivastava A, Lusby EW, Berns KI. Nucleotide sequence and organization of the adeno-associated virus 2 genome. J Virol. 1983;45:555–64. [PubMed: 6300419]

9. Chaudhary K, Moore H, Tandon A, Gupta S, Khanna R, Mohan RR. Nanotechnology and adeno-associated virus-based decorin gene therapy ameliorates peritoneal fibrosis. Am J Physiol Renal Physiol. 2014;307:F777–82. [PubMed: 25056353]

10. Igarashi T, Miyake K, Suzuki N, Kato K, Takahashi H, Ohara K, et al. New strategy for in vivo transgene expression in corneal epithelial progenitor cells. Curr Eye Res. 2002;24:46–50. [PubMed: 12187494]

11. Mohan RR, Schultz GS, Hong JW, Wilson SE. Gene transfer into rabbit keratocytes using AAV and lipid-mediated plasmid DNA vectors with a lamellar flap for stromal access. Exp Eye Res. 2003;76:373–83. [PubMed: 12573666]

12. Mohan RR, Sharma A, Netto MV, Sinha S, Wilson SE. Gene therapy in the cornea. Prog Retin Eye Res. 2005;24:537–59. [PubMed: 15955719]

13. Sharma A, Tovey JC, Ghosh A, Mohan RR. AAV serotype influences gene transfer in corneal stroma in vivo. Exp Eye Res. 2010;91:440–8. [PubMed: 20599959]

14. Mohan RR, Sharma A, Cebulko TC, Tandon A. Vector delivery technique affects gene transfer in the cornea in vivo. Mol Vis. 2010;16:2494–501. [PubMed: 21139995]

15. Mohan RR, Tovey JC, Sharma A, Schultz GS, Cowden JW, Tandon A. Targeted decorin gene therapy delivered with adeno-associated virus effectively retards corneal neovascularization in vivo. PLoS ONE. 2011;6:e26432. [PubMed: 22039486]

16. Mohan RR, Tandon A, Sharma A, Cowden JW, Tovey JC. Significant inhibition of corneal scarring in vivo with tissue-selective, targeted AAV5 decorin gene therapy. Invest Ophthalmol Vis Sci. 2011;52:4833–41. [PubMed: 21551414]

17. Mohan RR, Sinha S, Tandon A, Gupta R, Tovey JC, Sharma A. Efficacious and safe tissue-selective controlled gene therapy approaches for the cornea. PLoS ONE. 2011;6:e18771. [PubMed: 21533273]

18. Vance M, Llanga T, Bennett W, Woodard K, Murlidharan G, Chungfat N, et al. AAV gene therapy for MPS1-associated corneal blindness. Sci Rep. 2016;6:22131. [PubMed: 26899286]

19. Hippert C, Ibanes S, Serratrice N, Court F, Malecaze F, Kremer EJ, et al. Corneal transduction by intra-stromal injection of AAV vectors in vivo in the mouse and ex vivo in human explants. PLoS ONE. 2012;7:e35318. [PubMed: 22523585]

20. Tsai ML, Chen SL, Chou PI, Wen LY, Tsai RJ, Tsao YP. Inducible adeno-associated virus vector-delivered transgene expression in corneal endothelium. Invest Ophthalmol Vis Sci. 2002;43:751–7. [PubMed: 11867594]

21. Bogner B, Boye SL, Min SH, Peterson JJ, Ruan Q, Zhang Z, et al. Capsid mutated adeno-associated virus delivered to the anterior chamber results in efficient transduction of trabecular meshwork in mouse and rat. PLoS ONE. 2015;10:e0128759.

22. Buie LK, Rasmussen CA, Porterfield EC, Ramgolam VS, Choi VW, Markovic-Plese S, et al. Self-complementary AAV virus (scAAV) safe and long-term gene transfer in the trabecular meshwork of living rats and monkeys. Invest Ophthalmol Vis Sci. 2010;51:236–48. [PubMed: 19684004]

23. O'Callaghan J, Crosbie DE, Cassidy PS, Sherwood JM, Flügel-Koch C, Lütjen-Drecoll E, et al. Therapeutic potential of AAV-mediated MMP-3 secretion from corneal endothelium in treating glaucoma. Hum Mol Genet. 2017;26:1230–1246. [PubMed: 28158775]

24. Wang L, Xiao R, Andres-Mateos E, Vandenberghe LH. Single stranded adeno-associated virus achieves efficient gene transfer to anterior segment in the mouse eye. PLoS ONE. 2017;12:e0182473.

25. Thomas PB, Samant DM, Selvam S, Wei RH, Wang Y, Stevenson D, et al. Adeno-associated virus-mediated IL-10 gene transfer suppresses lacrimal gland immunopathology in a rabbit model of autoimmune dacryoadenitis. Invest Ophthalmol Vis Sci. 2010;51:5137–44. [PubMed: 20505195]

26. Cheng HC, Yeh SI, Tsao YP, Kuo PC. Subconjunctival injection of recombinant AAV-angiostatin ameliorates alkali burn induced corneal angiogenesis. Mol Vis. 2007;13:2344–52. [PubMed: 18199977]

27. Igarashi T, Miyake K, Asakawa N, Miyake N, Shimada T, Takahashi H. Direct comparison of administration routes for AAV8-mediated ocular gene therapy. Curr Eye Res. 2013;38:569–77. [PubMed: 23489150]

28. Lai LJ, Xiao X, Wu JH. Inhibition of corneal neovascularization with endostatin delivered by adeno-associated viral (AAV) vector in a mouse corneal injury model. J Biomed Sci. 2007;14:313–22. [PubMed: 17373573]

29. Nathwani AC, Tuddenham EG, Rangarajan S, Rosales C, McIntosh J, Linch DC, et al. Adenovirus-associated virus vector-mediated gene transfer in hemophilia B. New Engl J Med. 2011;365:2357–65. [PubMed: 22149959]

30. Nathwani AC, Nienhuis AW, Davidoff AM. Our journey to successful gene therapy for hemophilia B. Hum Gene Ther. 2014;25:923–6. [PubMed: 25397929]

31. The Szybalski W. 50th anniversary of gene therapy: beginnings and present realities. Gene. 2013;525:151–4. [PubMed: 23500596]

32. Schwartz AE, Rodrigues MM, Brown K, Gaskins R, Hackett J, Thomas G, et al. Corneal opacification in C57BL/6J mice. Cornea. 1982;1:195–204.

33. Koehn D, Meyer KJ, Syed NA, Anderson MG. Ketamine/xylazine-induced corneal damage in mice. PLoS ONE. 2015;10:e0132804.

34. Nathwani AC, Reiss UM, Tuddenham EG, Rosales C, Chowdary P, McIntosh J, et al. Long-term safety and efficacy of factor IX gene therapy in hemophilia B. New Engl J Med. 2014;371:1994–2004. [PubMed: 25409372]

35. Summerford C, Samulski RJ. Membrane-associated heparan sulfate proteoglycan is a receptor for adeno-associated virus type 2 virions. J Virol. 1998;72:1438–45. [PubMed: 9445046]

36. Qiu J, Mizukami H, Brown KE. Adeno-associated virus 2 coreceptors? Nat Med. 1999;5:467–8. [PubMed: 10229209]

37. Weller ML, Amornphimoltham P, Schmidt M, Wilson PA, Gutkind JS, Chiorini JA. Epidermal growth factor receptor is a coreceptor for adeno-associated virus serotype 6. Nat Med. 2010;16:662–4. [PubMed: 20473307]

38. Pillay S, Meyer NL, Puschnik AS, Davulcu O, Diep J, Ishikawa Y, et al. An essential receptor for adeno-associated virus infection. Nature. 2016;530:108–12. [PubMed: 26814968]

39. Akache B, Grimm D, Pandey K, Yant SR, Xu H, Kay MA. The 37/67-kilodalton laminin receptor is a receptor for adeno-associated virus serotypes 8, 2, 3, and 9. J Virol. 2006;80:9831–6. [PubMed: 16973587]

40. Mietzsch M, Broecker F, Reinhardt A, Seeberger PH, Heilbronn R. Differential adeno-associated virus serotype-specific interaction patterns with synthetic heparins and other glycans. J Virol. 2014;88:2991–3003. [PubMed: 24371066]

41. Wu Z, Miller E, Agbandje-McKenna M, Samulski RJ. Alpha2,3 andalpha2,6 N-linked sialic acids facilitate efficient binding and transduction by adeno-associated virus types 1 and 6. J Virol. 2006;80:9093–103. [PubMed: 16940521]

42. Kaludov N, Brown KE, Walters RW, Zabner J, Chiorini JA. Adeno-associated virus serotype 4 (AAV4) and AAV5 both require sialic acid binding for hemagglutination and efficient transduction but differ in sialic acid linkage specificity. J Virol. 2001;75:6884–93. [PubMed: 11435568]

43. Rocha EM, Di Pasquale G, Riveros PP, Quinn K, Handelman B, Chiorini JA. Transduction, tropism, and biodistribution of AAV vectors in the lacrimal gland. Invest Ophthalmol Vis Sci. 2011;52:9567–72. [PubMed: 22110082]

44. Li SK, Hao J, Liu H, Lee JH. MRI study of subconjunctival and intravitreal injections. J Pharm Sci. 2012;101:2353–63. [PubMed: 22473517]

45. Gaudana R, Ananthula HK, Parenky A, Mitra AK. Ocular drug delivery. AAPS J. 2010;12:348–60. [PubMed: 20437123]

46. Hewitt FC, Li C, Gray SJ, Cockrell S, Washburn M, Samulski RJ. Reducing the risk of adeno-associated virus (AAV) vector mobilization with AAV type 5 vectors. J Virol. 2009;83:3919–29. [PubMed: 19211760]

47. Li C, Goudy K, Hirsch M, Asokan A, Fan Y, Alexander J, et al. Cellular immune response to cryptic epitopes during therapeutic gene transfer. Proc Natl Acad Sci USA. 2009;106:10770–4. [PubMed: 19541644]

48. Li C, Hirsch M, DiPrimio N, Asokan A, Goudy K, Tisch R, et al. Cytotoxic-T-lymphocyte-mediated elimination of target cells transduced with engineered adeno-associated virus type 2 vector in vivo. J Virol. 2009;83:6817–24. [PubMed: 19369348]

49. Bennett J, Ashtari M, Wellman J, Marshall KA, Cyckowski LL, Chung DC, et al. AAV2 gene therapy readministration in three adults with congenital blindness. Sci Transl Med. 2012;4:120ra15.

50. Li Q, Miller R, Han PY, Pang J, Dinculescu A, Chiodo V, et al. Intraocular route of AAV2 vector administration defines humoral immune response and therapeutic potential. Mol Vis. 2008;14:1760–9. [PubMed: 18836574]

51. Amado D, Mingozzi F, Hui D, Bennicelli JL, Wei Z, Chen Y, et al. Safety and efficacy of subretinal readministration of a viral vector in large animals to treat congenital blindness. Sci Transl Med. 2010;2:21ra16.

52. Gilger BC. Immune relevant models for ocular inflammatory diseases. ILAR J. 2018:1–11. [PubMed: 31329902]

53. Hirsch ML, Conatser LM, Smith SM, Salmon JH, Wu J, Buglak NE, et al. AAV vector-meditated expression of HLA-G reduces injury-induced corneal vascularization, immune cell infiltration, and fibrosis. Sci Rep. 2017;7:17840. [PubMed: 29259248]

54. Song L, Li X, Jayandharan GR, Wang Y, Aslanidi GV, Ling C, et al. High-efficiency transduction of primary human hematopoietic stem cells and erythroid lineage-restricted expression by optimized AAV6 serotype vectors in vitro and in a murine xenograft model in vivo. PLoS ONE. 2013;8:e58757. [PubMed: 23516552]

55. Song L, Kauss MA, Kopin E, Chandra M, Ul-Hasan T, Miller E, et al. Optimizing the transduction efficiency of capsid-modified AAV6 serotype vectors in primary human hematopoietic stem cells in vitro and in a xenograft mouse model in vivo. Cytotherapy. 2013;15:986–98. [PubMed: 23830234]

56. Grieger JC, Choi VW, Samulski RJ. Production and characterization of adeno-associated viral vectors. Nat Protoc. 2006;1:1412–28. [PubMed: 17406430]

57. Llanga T, Nagy N, Conatser L, Dial C, Sutton RB, Hirsch ML. Structure-based designed nano-dysferlin significantly improves dysferlinopathy in BLA/J mice. Mol Ther. 2017; 25:2150–2162. [PubMed: 28629822]

58. Ye L, Yu H, Li C, Hirsch ML, Zhang L, Samulski RJ, et al. Adeno-associated virus vector mediated delivery of the HBV genome induces chronic hepatitis B virus infection and liver fibrosis in mice. PLoS ONE. 2015;10:e0130052.
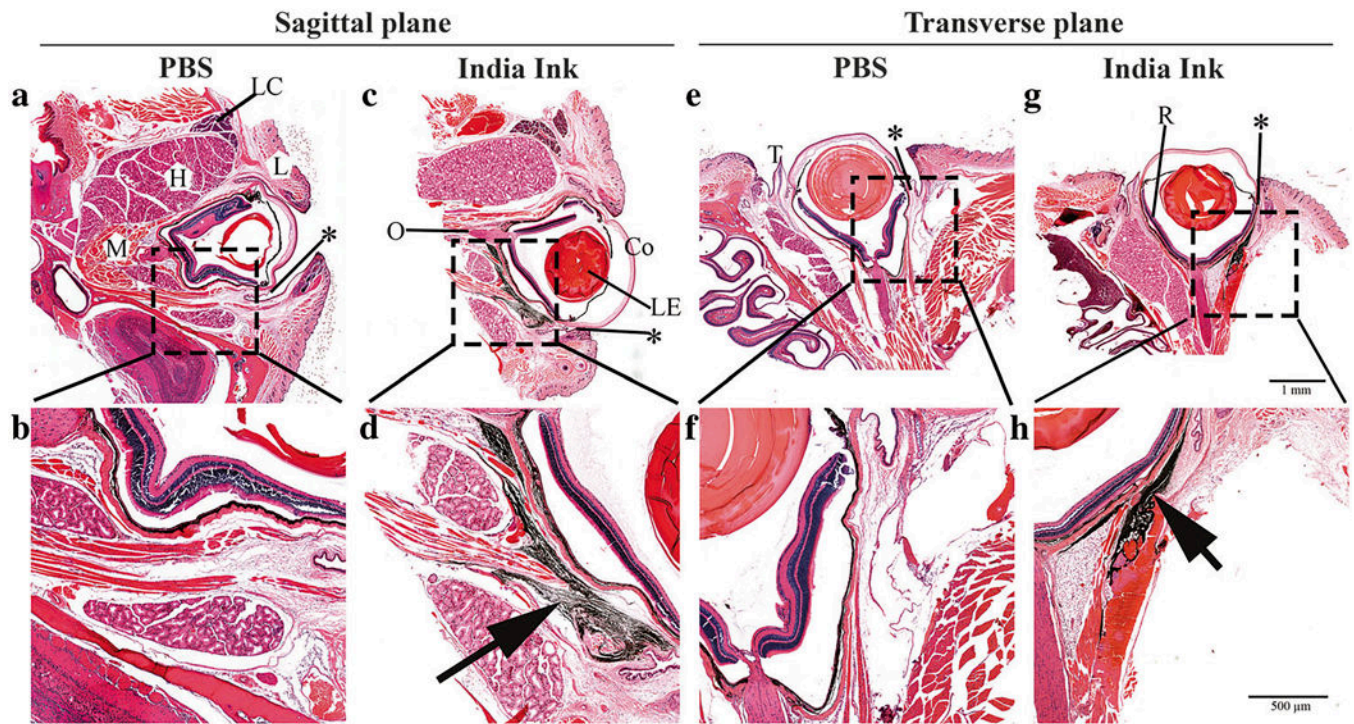
Fig. 1.
Histologic examination of the India ink distribution after subconjunctival injection in mouse eye. Sagittal plane (left panel) and transverse plane (right panel) of either PBS-injected (**a**, **b**, **e**, and **f**) or India ink-injected (**c**, **d**, **g**, and **h**) eye sections are presented. The injection site (asterisk) is located at the bulbar conjunctiva. L: eye lid, LC: lacrimal gland, H: harderian gland, M: muscle, LE: lens, Co: cornea, O: optic nerve, T: third eyelid, R: retina. The black staining (arrow) in the images indicate the localization of the India ink dispersion. Scale bar = 1 mm (upper) and 500 μm (lower)
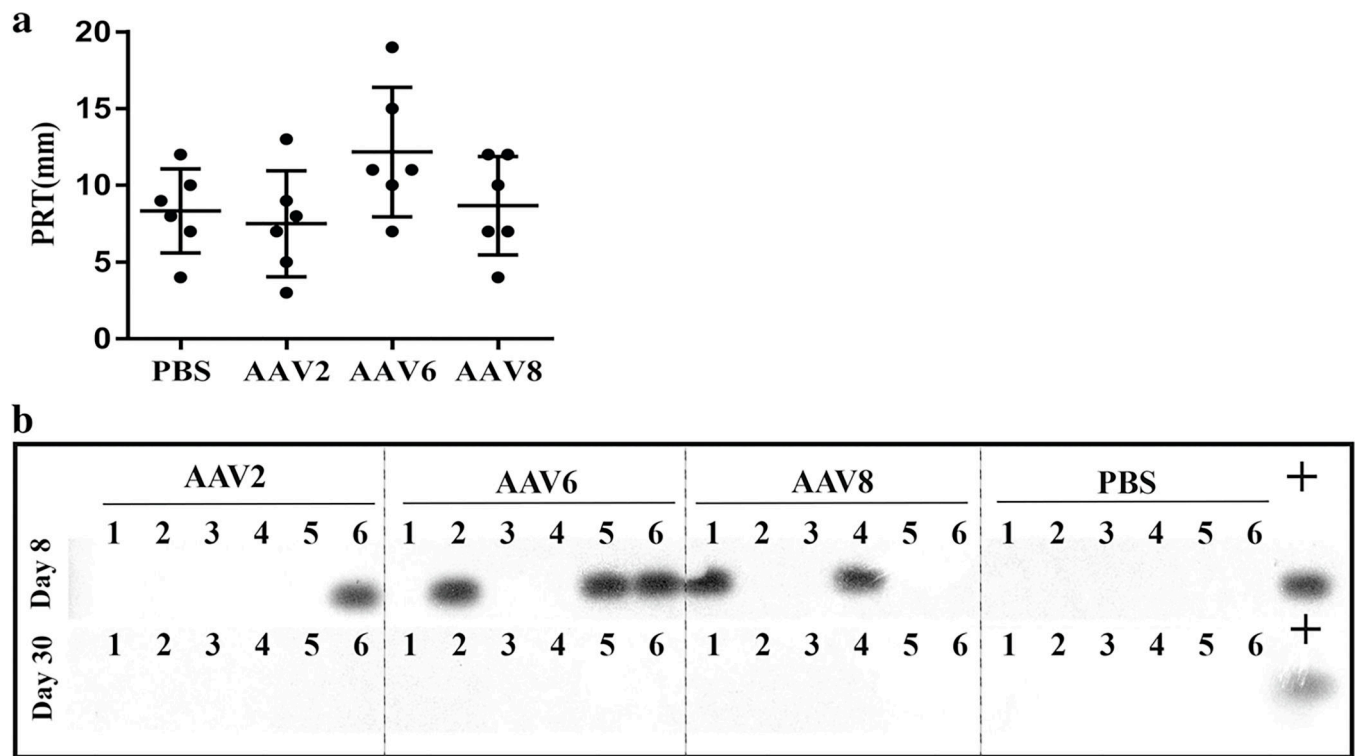
Fig. 2.
PRT tear production assay and vector shedding analysis. Tear production was measured by PRT test and data are presented as the length of wetted phenol red thread from each eye (**a**). To detect the vector shedded in tear, tear samples were collected at 1 week (**b**, upper panel) and 4 weeks (**b**, lower panel) after subconjunctival injection then subjected to two rounds of PCR using vector-specific primers sets and detected by a GFP-specific probe via Southern blotting. Viral vector genomes plus host cell gDNA was used as positive control template. The numbers 1–6 represent the individual tear samples (six eyes per group)
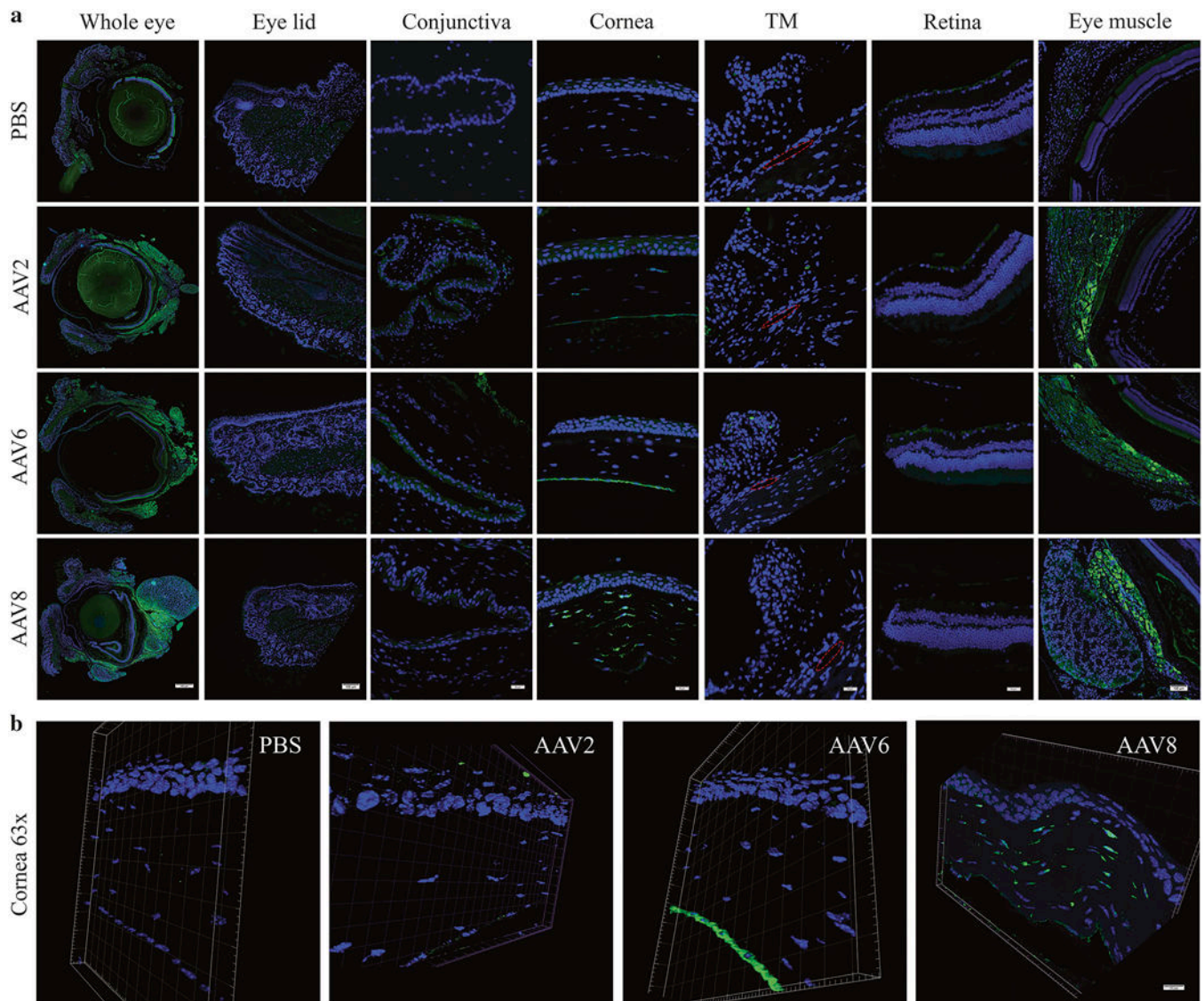
Fig. 3.

Representative histologic images of AAV-mediated GFP expression in different eye compartments. GFP expression (green) was examined by immunostaining with an anti-GFP antibody in paraffin-embedded tissue sections. Images spanning the entire thickness of the cross-sections of the whole eye or different eye compartments including eyelid, conjunctiva, cornea, trabecular meshwork, retina, and extraocular eye muscle as indicated (**a**) and representative confocal 3-D images at a 0.6-μm z-stack of cornea sections from the indicated mice (**b**) are presented. DNA staining by DAPI (blue). TM trabecular meshwork; red circle indicates the Schlemm's canal. Scale bar = 500 μm (whole eye in **a**), 100 μm (eyelid and eye muscle in **a**), 20 μm (conjunctiva, cornea, TM, retina in **a** and **b**)
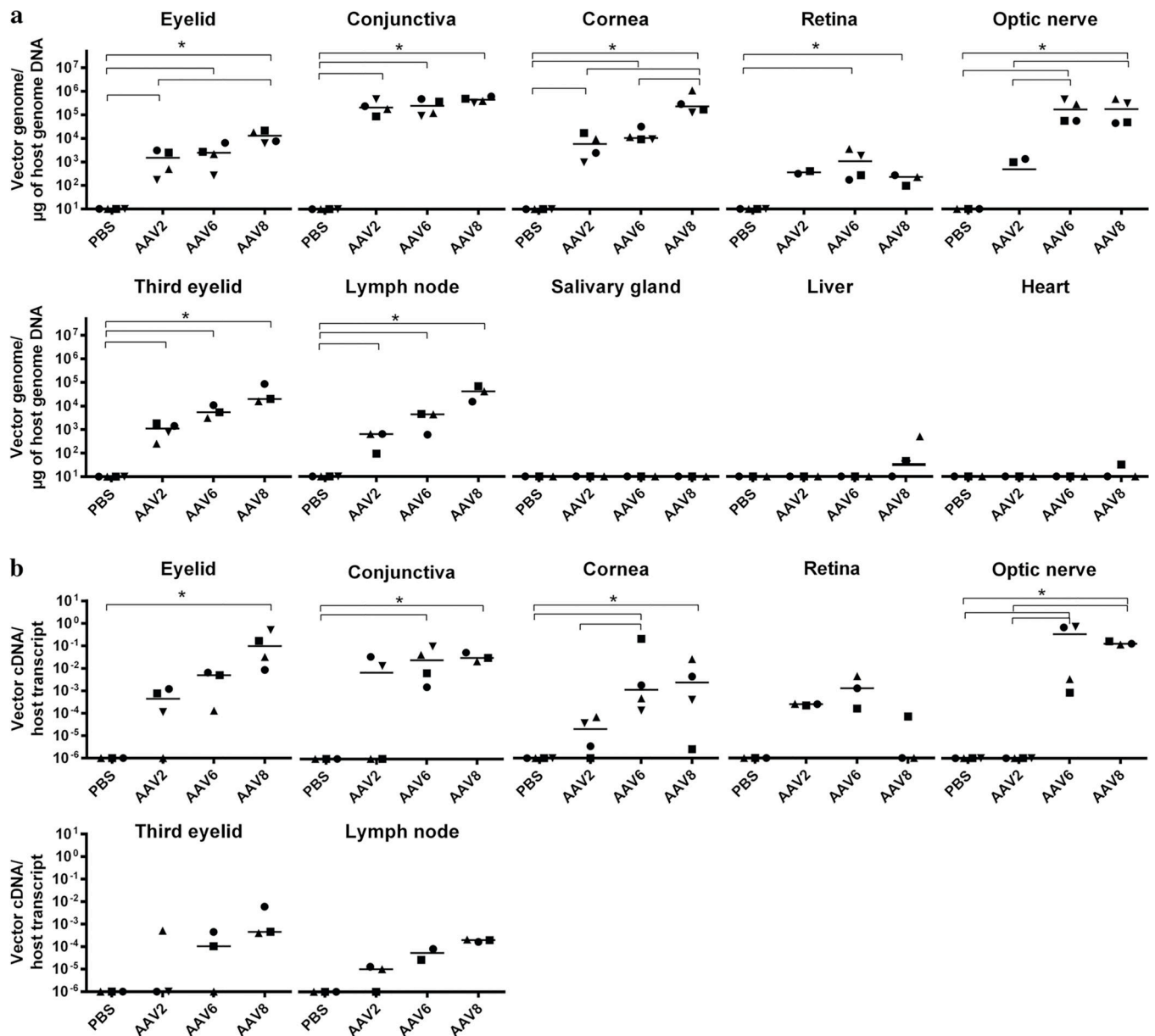
Fig. 4.

Quantitative analysis of vector biodistribution and transgene expression. Vector genome copy number in distinct eye compartments (eyelid, conjunctiva, cornea, retina, optic nerve, and third eyelid) as well as other organs (submandibular lymph nodes, salivary gland, liver, and heart) are shown as vector genome copy number/μg of host genome DNA (**a**); GFP abundance examination by qRT-PCR in selected tissues are presented as vector cDNA copy number/host transcript (**b**); * $p < 0.05$, Mann–Whitney test

a

Primary/Secondary receptor	HSPG	EGFR	37/67 KDa Lam R	AAVR	Sialic acid
Serotypes	AAV2, AAV3 AAV6	AAV6	AAV2, AAV3, AAV8, AAV9	AAV1, AAV2, AAV3B, AAV5, AAV6, AAV8, AAV9	AAV1, AAV4, AAV5, AAV6

b

c

		HSPG	EGFR	37/67KDa Lam R	AAVR	Sialic acid	α2, 3 Sialic acid	α2, 6 Sialic acid
Mouse	Ep	-	+	+	+	+	-	-
	St	-	-	+	+#	+	-	-
	En	+^	-	+	+	+	+	-
Human	Ep	+/-	+	+	+	+	-	-
	St	+/-	-	+	+#	+	-	-
	En	-	-	+	+	+	+	-
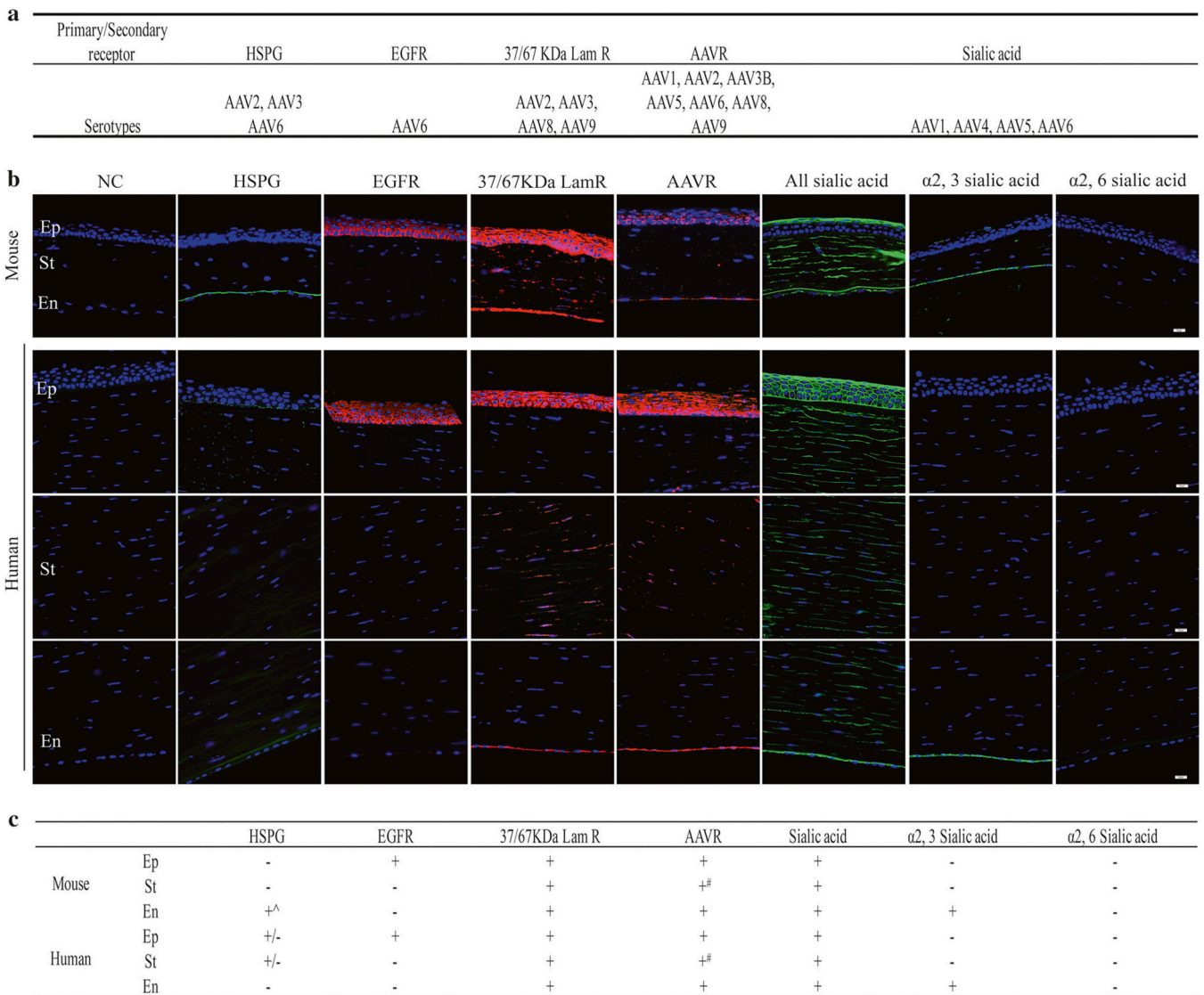
^: Positive at the Endothelium-Descemet's layer interface; +/-: Inconclusive; #: Weak positive, needs longer exposure time.

Fig. 5.

AAV receptor analysis of mouse and human cornea by immunofluorescence staining. Selected AAV primary/secondary receptors analyzed in the present study are listed in (**a**). anti-HS antibody, anti-EGFR antibody, anti-67 kDa Lam R antibody (recognizes both 37 kDa Lam R precursor and 67 kDa Lam R), and anti-AAVR antibody were used for HSPG, EGFR, 37/67 kDa Lam R, and AAVR staining in mouse cornea and human cornea, respectively. WGA, SNA, and MAL I were used for staining of multivalent sialic acid, α2, 6 sialic acid, and α2, 3 sialic acid, respectively. Three individual images of human cornea for each section are presented to show the epithelium, stromal, and endothelium layer, respectively. NC negative control (no primary antibody), Ep epithelial layer, St stromal layer, En endothelial layer. Scale bar = 20 μm

Table 1

Neutralizing antibody assay

Serum	Neutralizing antibody titer	Vector serotype tested in assay
PBS_Mouse 1	ND	AAV2
PBS_Mouse 2	ND	AAV6
PBS_Mouse 3	ND	AAV8
AAV2_Mouse 1	2048	AAV2
AAV2_Mouse 2	2048	AAV2
AAV6_Mouse 1	1024	AAV6
AAV6_Mouse 2	512	AAV6
AAV6_Mouse 3	256	AAV6
AAV8_Mouse 1	256	AAV8
AAV8_Mouse 2	128	AAV8
AAV8_Mouse 3	256	AAV8

Mouse 3 in the AAV2 group was excluded due to insufficient serum volume for the assay

The neutralizing antibody titer as 50% of transduction inhibition was listed for each mouse

ND not detectable